

Halgren E. Considerations in Source Estimation of the P3. In: Ikeda I, Inoue Y, eds. *Event-related Potentials in Patients with Epilepsy: from Current State to Future Prospects*. Paris: John Libbey Eurotext 2008: 71-87.

## Considerations in Source Estimation of the P3

Eric Halgren, Ph.D.

Multimodal Imaging Laboratory

Departments of Radiology, Neurosciences and Psychiatry, University of California at San Diego

### Abstract

It is not possible to localize the cerebral structures that generate the P3 from non-invasive recordings. In addition to inherent ambiguities in source localization, many generators that are active during the P3 do not propagate to the scalp and thus would remain invisible to even perfect inverse solutions. Furthermore, scalp recordings are not directly informative with regard to underlying neural processes. In theory, fMRI could help distinguish between alternative P3 generators, but in practice, its utility may be limited. Recordings directly within the brain are limited by incomplete sampling and possible pathology. However, they are the only unambiguous means to demonstrate local generation of potentials which overlap in time with the scalp P3 and possess similar cognitive correlates. Decreases in scalp P3 after brain lesions suggest which structures might contribute directly to the scalp P3, but post-lesion decreases can also be due to disruption of antecedent calculations. Despite these considerations, and remaining dissociations, there is increasing convergence in the distribution of generator structures inferred from different methods. However, bringing the P3s and the cognitive states that they embody into mechanistic neuroscience requires going beyond the localization of generating structures to identifying generating synapses, channels and circuits.

key words: P300, event-related potentials, cortex, humans, inverse problem, generators, thalamus, slow oscillation, sleep spindle

### Even a perfect inverse solution cannot localize what it does not see

It is impossible to unambiguously localize the structures generating the P3 from extracranial recordings for two fundamental reasons that are inherent in the biophysics of EEG and MEG, and can never be overcome by advances in analysis techniques. First, the inverse problem is ill-posed: there are an infinite number of cortical activation patterns that could result in any recorded scalp-P3 topography. Second, most of the brain generators active during the P3 do not propagate to the scalp to produce a recordable potential due to spatiotemporal cancellation. Fortunately, under some circumstances, intracranial EEG (iEEG) recordings *can* unambiguously localize P3 generators. Such recordings have made it clear that the P3 actually refers to several states, with different generating structures and evoking circumstances. These studies, reviewed in the companion chapter by Halgren in this volume, serve as a touchstone for evaluating the non-invasive techniques.

### Neural processes generating EEG and MEG

The underlying P3 process can be measured with a variety of techniques, each of which can provide complementary insights. EEG, MEG and the blood oxygenation level dependent (BOLD) response measured with functional MRI are all closely related to synaptic transmission and transmembrane currents (fig. 1). Ionic concentration gradients act as batteries, driving current actively across the membrane, and drawing it from, or pushing it into, the intracellular and extracellular spaces. Aligned intracellular currents are thought to comprise the main generators of MEG [1], whereas aligned extracellular currents are measured as EEG [2]. The intracellular and extracellular currents are equal and passive, and result directly from the same active current flows across neuronal membranes. Consequently, the EEG and MEG share the same active generators but propagate differently to their respective sensors. Thus, they provide complementary localizing information [3,4]. BOLD functions to support the energy needs of the brain, and in primates these are mainly related to synaptic processes and consequent currents [5]. This is the fundamental reason to expect that EEG and MEG measures of the P3 would be highly similar to each other, and at least partially share a generating substrate with the BOLD response in the same task. However, there are also many ways in which these measures could be dissociated, which we shall consider below.

On the one hand, generation of the EEG (and thus event-related averages of the EEG, and thus the scalp-P3) is very simple: active currents flow across cell membranes in the brain, and these currents then flow through the extracellular space, thus producing potential differences between electrodes at different locations on the scalp. On the other hand, there are many kinds of active currents in the brain, each of which has its own biological context and function [6]. The spatial arrangement of these currents and the paths they take are incredibly complex, as is the spatiotemporal choreography of their activation. Fortunately, biophysical considerations applied to the biology of these currents allow one to understand which of them are likely to contribute to the EEG. In most cases the same considerations apply equally to MEG and they will be discussed together.

**Action potentials**

Action potentials contribute little to the M/EEG signal for several reasons [7]. First, the action potential is organized as a central current sink surrounded by sources. Current crosses the axonal membrane behind the active sink to restore its resting potential. Current is drawn from in front of the spike to supply charge to the active sink. Consequently the action potential is equivalent to a quadripole which decreases with distance much faster than do the equivalent dipoles produced by synaptic activation. Second, axonal diameters are generally small compared to dendritic, and so the currents involved are small (and are even smaller for myelinated axons due to saltatory conduction). Third, action potentials are very short and biphasic so tend to cancel due to temporal asynchrony; even a half millisecond offset can result in cancellation whereas waves as long as the P3 (~200ms) will summate even when offset by 100ms. Fourth, axons tend to form tangles resulting in spatial cancellation (rather than palisades like apical dendrites). Fifth, the return currents are close to the primary sinks (especially for action potentials in unmyelinated axons, the most common in the cortex itself) so the dipoles are short and thus weak. There are apparent exceptions, such as the primary somatosensory cortex response to median nerve stimulation [8], but these provide a very weak signal that is only apparent because it is the first cortical response and thousands of trials are averaged.

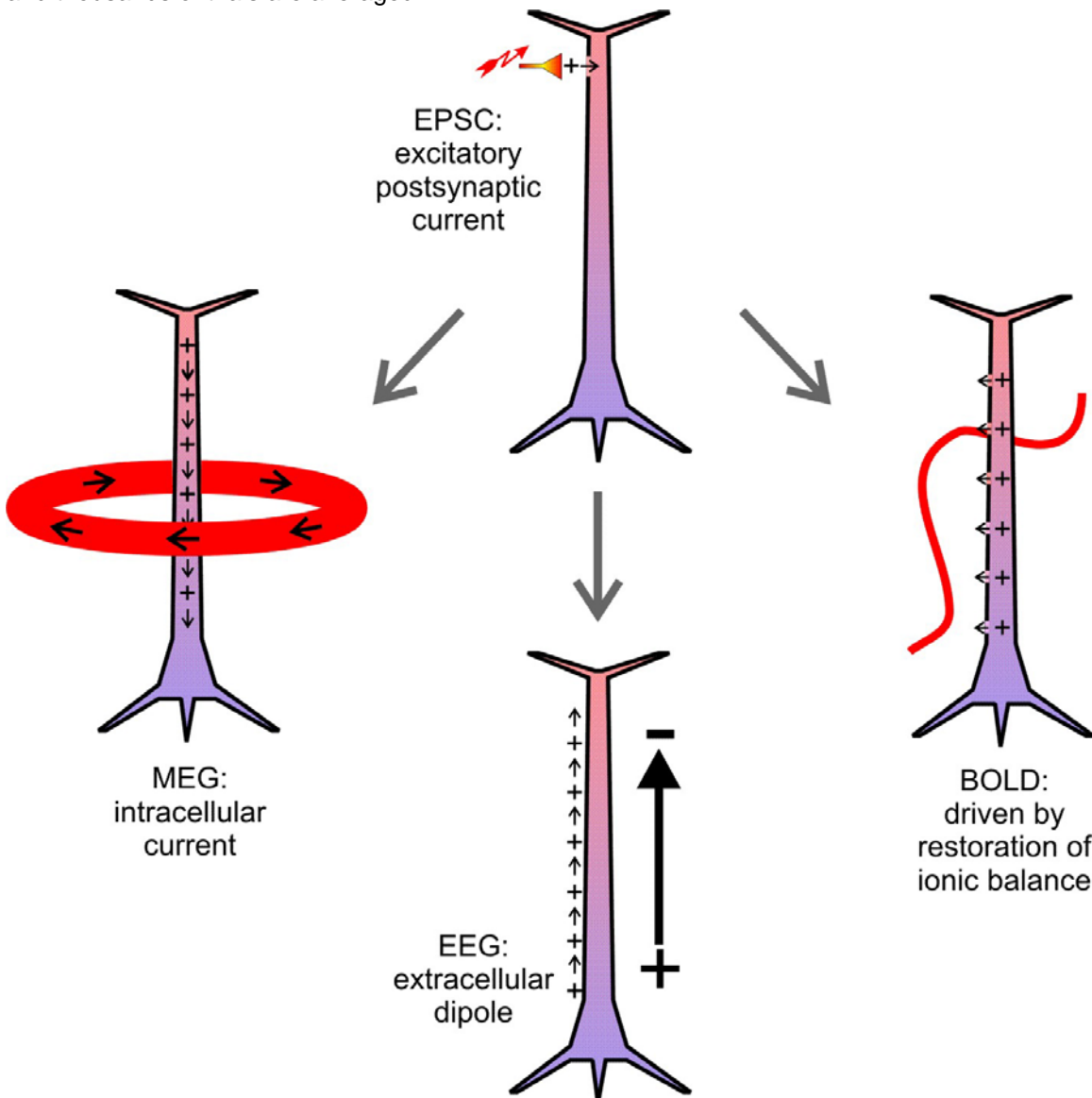


**Figure 1. Common Origin of MEG, EEG and BOLD in Active Transmembrane Currents.** The excitatory postsynaptic current (EPSC) induced by the opening of ligand-gated channels in the postsynaptic membrane (shown at top at the distal apical shaft of a cortical pyramidal cell), results in an intracellular current (left) which when summated across many cells generates the MEG. The equal but opposite extracellular return current results in the EEG (bottom), and restoring ionic balance through active pumping is a major driving force behind the BOLD response (right).

### ***Inhibition***

It has been controversial if inhibitory currents also contribute to M/EEG. A major reason for this doubt has been that GABA<sub>A</sub> receptors function by permitting Cl<sup>-</sup> ions to pass, and the reversal potential of chloride (-71 mV) had been thought to be similar to the resting potential of cortical pyramidal cells [9]. Increased Cl<sup>-</sup> conductance would shunt current arriving at the soma and prevent it from triggering an action potential, thus inhibiting neurons without affecting their membrane potential. Even if this were the case, however, the shunting current would still alter the dipole produced by simultaneous EPSP in the apical dendrites of the same cell by increasing the separation between its poles. This increased dipole length would result in a proportionate increase in dipole strength. Furthermore, the supposedly hyperpolarized state of resting cortical cells was based on measurements in anesthetized animals or slices. More recent data in awake animals find resting potentials of ~-63 mV, i.e., depolarized from the equilibrium potential of Cl<sup>-</sup> [10]. Finally, GABA<sub>B</sub> receptors which appear to predominate in associative interactions in the cortex [11] operate mainly via K<sup>+</sup> currents, which reverse at -89 mV, far removed from the resting potential. Intrinsic voltage-gated K<sup>+</sup> channels are also major contributors to the active currents that have been shown to be major contributors to delta waves [12].

At the circuit level, it appears that inhibition and excitation are largely simultaneous and correlated, especially at the time scale of the P3. The concept of recurrent inhibition holds that a strong excitation would be followed by recurrent inhibition [13]. It had been thought that recurrent inhibition provided a good model for evoked potentials as well as spontaneous EEG. However, it is now appreciated that especially in cortical associative circuits, long-lasting polysynaptic excitation of AMPA and NMDA glutamate receptors are balanced by feedforward GABA<sub>B</sub> inhibition [14].

### ***Voltage-gated channels***

Thus far we have mainly discussed the possible contributions to M/EEG of traditional ligand-gated channels that are opened by the binding of a specific neurotransmitter at post-synaptic sites, and of fast voltage-gated channels producing axon potentials. Voltage-gated channels also occur in the soma and dendrites, with slow time-constants comparable to the frequencies present in the P3 [15]. These later channels are known to play a dominant role in producing certain spontaneous slow M/EEG phenomena (see below). Murakami and Okada examined the relative contribution of different channels to local field potentials (LFP) and MEG signals produced by the transverse hippocampal slice *in vitro* [16,17]. Channel activity was modeled using the detailed mathematical model of Traub [18], as guided by simultaneous intracellular recordings and estimates from the literature. They found that most of the M/EEG signal evoked by local stimulation was due to voltage-gated rather than ligand-gated channels.

In summary, M/EEG result from voltage- and ligand-gated currents across dendrosomatic membranes. The batteries powering these currents are the potential differences (or equivalently the ionic concentration differences) across cell membranes. These currents take very short paths and so produce tiny dipoles; they are perpendicular to the cell membrane thus cancel across the different sides of a dendritic cross-section; consequently they are not directly seen with MEG or EEG, although they are the ultimate source of both. After crossing the cell membrane, current will distribute itself within the neuron according to the resistance of the different paths open to it, which is determined by the shape of the cell [19].

## **Spatiotemporal cancellation during passive propagation of the M/EEG**

### ***Spatial cancellation***

It appears that in most cases, the intracellular and extracellular currents resulting from transmembrane currents are spatially disorganized so that no significant net dipole is produced (fig. 2). Pyramidal cells, however, possess four unusual characteristics that guide the net currents flowing to and from the channels on their surface to often summate and produce M/EEG (fig. 1). First, pyramidal cells possess a prominent and long apical dendrite. If the active current enters the cell at the tip of the apical dendrite, it will tend to flow down the large apical shaft toward the soma rather than into tiny terminal dendritic branches. This internal current produces the MEG signal. The internal current releases charge on the outside of the membrane that then flows back to the active site, and this external polarized current results in the EEG. Pyramidal cells are unusual in this morphology that guides net intracellular and thus extracellular current in a single long line; currents in stellate cells, and even the basal dendrites of pyramidal cells would tend to flow in many radial lines and thus produce no net dipole. Second, pyramidal cell apical dendrites are aligned so their currents run in parallel; further the apical dendrites of a given pyramidal cell population begin and end in relatively restricted layers so that the currents begin and end together. Together this organization results in the individual currents summing across pyramidal cells. Third, pyramidal cells are the most numerous of all cortical neurons (~70%), and thus their summated currents will be relatively large. Fourth, the intracolumnar as well as external connections of pyramidal cells are arranged in layers, or lamina. For example, different lamina are targeted by feedforward vs feedback distant cortico-cortical connections [20,21], by characteristic connections between cortical layers [22], and by core vs matrix thalamo-cortical connections [23]. Thus, synaptic input from a given source is localized to a discrete portion of the dendrite and the resulting currents are spatially aligned in parallel with the apical dendrites, perpendicular to the cortical surface. These four spatial properties are ultimately the byproduct of the phased developmental program that constructs the cerebral cortex [24]; if any were lacking

the M/EEG would be much smaller and probably rather uninteresting.

Apical dendrites are essentially parallel only on a small scale of <1cm, at larger distances they may point away from each other due to the highly folded nature of the human cortex. Quite often, the dipoles lie on opposite sides of a sulcus, in which case they will largely cancel. In such situations, lesions of one side of the sulcus would result in an increased signal due to decreased cancellation. Much of the hippocampal fields may cancel due to its tubular structure. Although as reviewed above, numerous groups have found large P3b's generated in the hippocampus, lesions of the hippocampus have little or no effect on the scalp-P3b [25-28]. Unpublished simulations (Ahlfors et al) show that at reasonable levels of brain activity (~10% of the cortical surface active), most (>90%) of the M/EEG response at the sensors is cancelled compared to what would be recorded when each is activated individually. When a complex arrangement of cortical sources in a given area do not completely cancel, they will always appear as a simple dipolar pattern at a sufficient distance because the dipolar term drops off more slowly with distance [29]. In the simplest example, a focal source may produce an external pattern that is indistinguishable from activation distributed over a broader area [30,31]. Requiring a high 'goodness-of-fit' does not address this problem, as it is often excellent for erroneous single dipole models for complex generating sources [32]. All of the above ways in which transmembrane currents may fail to result in an extracranial signal apply equally to MEG and to EEG. MEG has an additional blindness: radial sources produce very small extracranial MEG fields that may not rise above the noise [33,34]. Thus, as measured outside the head, it is easy to imagine complex arrangements of dipoles that cancel each other except for a residual that can appear as a small dipole at a distance.

### **Temporal cancellation**

Spatial organization is thus necessary for transmembrane currents to produce summing dipoles. However, it is not sufficient. If the dipoles from individual cells or groups of cells are asynchronous with those in overlapping groups, then they will also tend to cancel each other [35]. Optimal propagation will be achieved by relatively slow synaptic activations synchronized over large areas of the cortex by the thalamus, brainstem or cortico-cortical fibers. These synchronizing mechanisms become manifest in spontaneous rhythms, which we discuss in the companion chapter by Halgren. Here, we turn to other methods for localizing the P3 generators.

### **Limits of perfection**

If a given neural activity fails to produce an extracranial signal, then it cannot be detected regardless of the accuracy of the inverse method applied to the extracranial signal. For these reasons, the '*origin of the M/EEG signal,*' and the '*brain activity indexed by the M/EEG signal,*' are not at all the same thing. While from a technical viewpoint, the goal of source modeling is to find out what brain area is generating the recorded signals, the neurophysiologist rather seeks to infer the activity patterns present in the brain regardless of whether they propagate extracranially. Since most transmembrane currents probably do not result in an M/EEG signal, these are very different questions. We may hope that when the P3 is understood in terms of its underlying neuronal systems, then extracranial recordings can be used as an index or marker of the system, rather than as a method capable of exhaustive and certain detection of its generating component structures.

### **Disambiguation of M/EEG source localization with BOLD**

M/EEG reflect the transmembrane currents in the brain instantaneously; they thus have temporal resolution limited only by their sampling rate and directly reflect neuronal information processing. However, certain localization of M/EEG from extracranial sensors is physically impossible [36]. Localization of the BOLD response is certain, but it has a delayed and uncertain relationship to neuronal information processing. The problem with M/EEG source localization is not that there is a lack of spatial information, but that it is ambiguous: prior assumptions are needed to choose among the infinite number of possible source configurations that could have produced the observed signal topography. Since BOLD is not ambiguous and comes from a biologically related source, it has been used as a prior assumption.

### **Neural processes generating BOLD responses**

Like M/EEG, BOLD does appear to be influenced by inhibition as well as excitation. In rat barrel cortex [37] and primate visual cortex [38], surround neuronal inhibition is associated with decreased BOLD. Also like M/EEG, BOLD does not appear to be directly sensitive to action potentials. Within the cerebellum, rCPF changes can be easily dissociated from the firing of its principle neurons, the Purkinje cells [39]. Attwell and Iadecola [40] estimated that action potentials in nonhuman primates utilize ~10% of the brain's energy budget, whereas postsynaptic processes consume ~75%. Although the relatively small amount of energy used by action potentials would argue against neuronal firing being the critical factor controlling the hemodynamic response, this is an indirect argument; recent evidence suggests that the hemodynamic response is controlled by signals from particular cell groups, rather than by a net sampling of energy metabolism. For example, measurement with PET of rCBF in response to visual stimulation found that increasing the distance from metabolic normalcy with hypoxia did not increase the rCBF response [41]. Several neurovascular control systems have been identified, including extrinsic nerves from the peripheral nervous system innervating pial vessels [42]. Within the central nervous system, cholinergic, serotonergic, noradrenergic, and other neuromodulatory systems innervate microvessels within the cortex, transduced through astrocytes and interneurons, forming neurovascular units acting via

nitric oxide and other vasoactive mediators [42]. A critical role for interneurons in the neurovascular control system is also suggested by the observation *in vitro* that activation of single interneurons can evoke visible changes in cortical microvessels [43].

### **Associations and dissociations between M/EEG and BOLD**

The above discussion provides several reasons why M/EEG and BOLD may be generated by the same places and neural activities. Ultimately, these measurements reflect the same fundamental main driving force: the transmembrane dendrosomatic currents that directly give rise to the MEG and EEG (as their intracellular and extracellular limbs, respectively), are also the brain's main energy consumer and thus produce the deficit that the hemodynamic response seeks to restore. Further, both M/EEG and BOLD can reflect either inhibitory or excitatory dendritic currents, but receive relatively little contribution from action potentials *per se*. These considerations explain the tight coupling sometimes observed between electromagnetic and hemodynamic cortical changes [44,45].

On the other hand there are important differences in how the dendrosomatic currents come to be reflected in measurements at the sensors that might lead to quantitative and qualitative dissociations. On the way from the neuronal membrane to M/EEG sensor, most transmembrane currents are probably lost to spatial cancellation and temporal asynchrony. Conversely, the hemodynamic response is not directly controlled by the energy state of the brain, but by control mechanisms that are likely to be invisible to M/EEG: the interneurons that may be the final common pathway in the neurovascular control circuit are stellate cells whose geometry would not produce significant propagating dipoles, nor would perivascular contacts. However, the cholinergic and monoaminergic control pathways that modulate the neurovascular response may be the same ones that control the state of the thalamocortical circuits that underlie M/EEG synchrony, potentially leading to an overall correlation between these rhythms and cerebrovascular tonus.

In conclusion, although both M/EEG and fMRI/PET probably mainly reflect dendrosomatic transmembrane currents, not much can be directly inferred from either regarding the synapses or channels involved. There are some strong reasons why M/EEG and fMRI/PET might reflect either highly similar or very different neuronal activity, depending on the circumstances. The particulars of the M/EEG and fMRI/PET neural bases and of their relations with each other are likely to vary in different tasks, locations, latencies, measures, states and species, within different physiological systems. Thus, although their general relationship permits BOLD to be used to predict the M/EEG, it is too variable to use methods that force or assume too strong a relationship.

### **Strategies for combining BOLD and M/EEG even when they are not perfectly correlated**

Specific strategies can be applied to minimize the effects of potential dissociations between M/EEG and BOLD. Suppose, for example, that the underlying neural response as well as its M/EEG manifestation was equal but latency-shifted across two comparison conditions. Then the BOLD response, lacking temporal resolution, would fail to observe any difference, whereas the M/EEG response would be markedly different, especially in subtraction waveforms. If one were to use only the areas showing differential BOLD responses as priors for localizing the M/EEG difference waveform, then crucial areas would be lacking. This problem would be avoided by including all areas showing a BOLD difference in any task comparison to baseline as priors. Simulation studies have shown that the disambiguating power of BOLD priors is little affected by including too many areas, but is severely weakened by including too few [3].

The poor temporal resolution of BOLD is also problematic because it is unable to distinguish generators of the P3 from other waves that are closely associated with it. Specifically, the same situations that evoke the P3b also evoke antecedent activity (partially reflected in the N2b) that may very well not be in the same location, but that fMRI cannot distinguish. Indeed, the antecedent processing may be more likely to be associated with increased neuronal activity and thus increased BOLD than the P3b which may sometimes be related to inhibition (see companion chapter by Halgren). This concern is smaller for the P3a because, although intracranial recordings show it is associated with a preceding MMN/N2a and followed by a SWa in a typically triphasic waveform, this association appears to be true everywhere that the P3a is recorded. Thus, even if the BOLD increase during trials that evoke the P3a is actually evoked by neural activity underlying the N2a, that is not important because the N2a and P3a appear to be co-localized.

A second situation where BOLD and M/EEG may dissociate is when weak synchronous inhibition produces large M/EEG signals but a decrease in metabolism. The influence of synchrony is so powerful [46] that it is easy to imagine it resulting in situations where an *increase* in M/EEG being associated with a *decrease* in fMRI. For example, the largest EEG waves are the 0.5-4 Hz activity during slow wave sleep produced by thalamocortical mechanisms that have been well-studied in animals [47]. These large waves are associated with greatly reduced synaptic activity and decreased metabolism [48]. Thus, it is essential to include as priors areas with decreased as well as increased BOLD, and to accept that BOLD and M/EEG may not be monotonically related.

A particularly egregious problem in using BOLD to localize the P3b is that powerful generators identified with intracranial recordings are in anteroventral temporal lobe structures that are especially prone to fMRI susceptibility artifacts [49,50]. In addition to methods that can partially recover signal in these areas, one can choose a relatively low significance threshold for the fMRI. Again, since this allows the inclusion of the maximum number of candidate areas, the choice of a threshold as high as  $p < .1$  can be considered as the most conservative approach. Of course, this strategy will

not work if these areas have been lost entirely due to the slice prescription, a problem especially of PET studies. Regardless of the strategy employed, some M/EEG generators will likely escape detection with fMRI. Simulation studies indicate that this can lead to grossly inaccurate source solutions, if the M/EEG generators are forced to one of the remaining candidates; conversely little price in source localization is paid if the source localization is only partially biased toward the areas identified with BOLD [3].

### ***Focality and synchrony as priors for source localization from M/EEG***

Keeping these strategies in mind, the information from structural and functional MRI can be used as priors to select between alternative generator configurations permitted by the M/EEG topography. These methods differ in the additional priors that are applied to solve the inverse problem, typically concerning the degree of focality and synchrony of the generators. For example, the extracranial-P3 is often modeled with a single or a few pairs of equivalent current dipoles (ECDs) [51]. The high level of focality implicit in this approach is seemingly at odds with the many regions that have been shown to be active during the P3 [52]. More generally, iEEG recordings have clearly shown that during cognitive tasks, many areas become rapidly engaged, and remain engaged in an overlapping and distributed fashion [53,54]. This is reasonable given that auditory and somatosensory input arrive at the cortex by ~20ms, and visual by ~60ms after stimulus onset, and it takes <~15 ms for any location in the cortex to communicate with any other [55,56]. Thus, by the time of the P3, ample time has passed for the entire cortex to be active for a long period, when considering only cortico-cortical connections. In addition, projections from modulatory structures in the thalamus, basal forebrain, and brainstem are available to synchronize brainstates across the cortex. If the P3 generators are related to those of spontaneous EEG oscillations, then widespread generation would be expected since these processes are characteristic of the cortex as a whole. Finally, the cognitive correlates of the P3, such as context updating and orienting, would be expected to be processing states that involve large parts of the cortex.

It is sometimes argued that fMRI studies have demonstrated that cognitive brain activations are highly focal. However, focality in BOLD responses may reflect the analysis strategy rather than the underlying neurobiology. BOLD analysis often shows only clusters of activation and/or require stringent statistical thresholds in order to overcome false positives due to the large number of voxels being examined for responses. When higher sensitivity is achieved by averaging large numbers of subjects, situations that evoke the scalp-P3 are found to evoke very widespread and extended activity even at very stringent thresholds [57].

Focal ECDs would still be quite useful if they could be relied upon to be located near the centers of generating regions. Indeed, if the generating region is relatively small (on the order of a few square cm<sup>2</sup>), this may be true [30,31]. However, when large regions are activated, as may very well be the case with the P3, an ECD may represent active cortex that is several cm distant, precluding meaningful interpretation.

Partly in response to such considerations, methods for estimating distributed source distributions have been developed [58]. Each of these contains, usually implicitly, assumptions regarding the focality of the underlying neuronal generators. For example, minimum current estimates (L1 norm) assume that the brain minimizes current in distributing sources across the cortical surface [59,60], whereas the minimum norm (L2 norm) assumes that the brain minimizes power [61,62]. Consequently, minimum current estimates will be more focal than minimum norm estimates for purely mathematical reasons that have no rationale in neurobiology (there is no reason to suppose that the brain minimizes either the amount of current or the amount of power it uses in producing an extracranial signal). Given what we know of the P3 generators from iEEG, one might choose assumptions that encourage highly distributed solutions [63], but again it is important to realize that these assumptions are unproved. While it is clear that the P3a and P3b are each generated in many cortical areas, it is not clear how distributed their generators are within each area, due to the sparse sampling of most iEEG recordings (see below).

Other methods for constraining source solutions begin with the extraction of statistically independent components of the signals present at the M/EEG sensors [64-66]. These components have a spatial topography, which can be localized with the same techniques as the original signals. However, as noted above, similar P3s can be recorded at multiple intracranial locations- thus they are clearly not independent of each other. Unaveraged iEEG also shows a fairly high level of coherence both at relatively short distances [67], as well as at longer ranges, with average coherence measures of about .35 [68]. These coherences can transiently increase dramatically across the cortex during information processing [68].

In summary, source localization from M/EEG *requires* prior assumptions. These may include the assumption that the M/EEG is generated by dipoles that are: (1) in the cortex and perpendicular to its surface; (2) in the same locations as BOLD increases in the same tasks and conditions; (3) focal or distributed; (4) few or many in number; and (5) statistically independent. While generating dipoles are likely to be in the cortex, the distribution of BOLD responses only provides a partial guess that might help choose among candidate generators. Basic cortical anatomy and physiology, as well as BOLD and iEEG recordings strongly imply that the P3 is not generated by a few focal generators. Rather than independent sources, iEEG finds that the timecourses of different cortical sources are highly similar. In any case, no set of prior assumptions are known with enough certainty to permit confident localization of the P3 from extracranial recordings. Thus, their implications need to be validated with iEEG, as it can sometimes provide certain localization of generators.



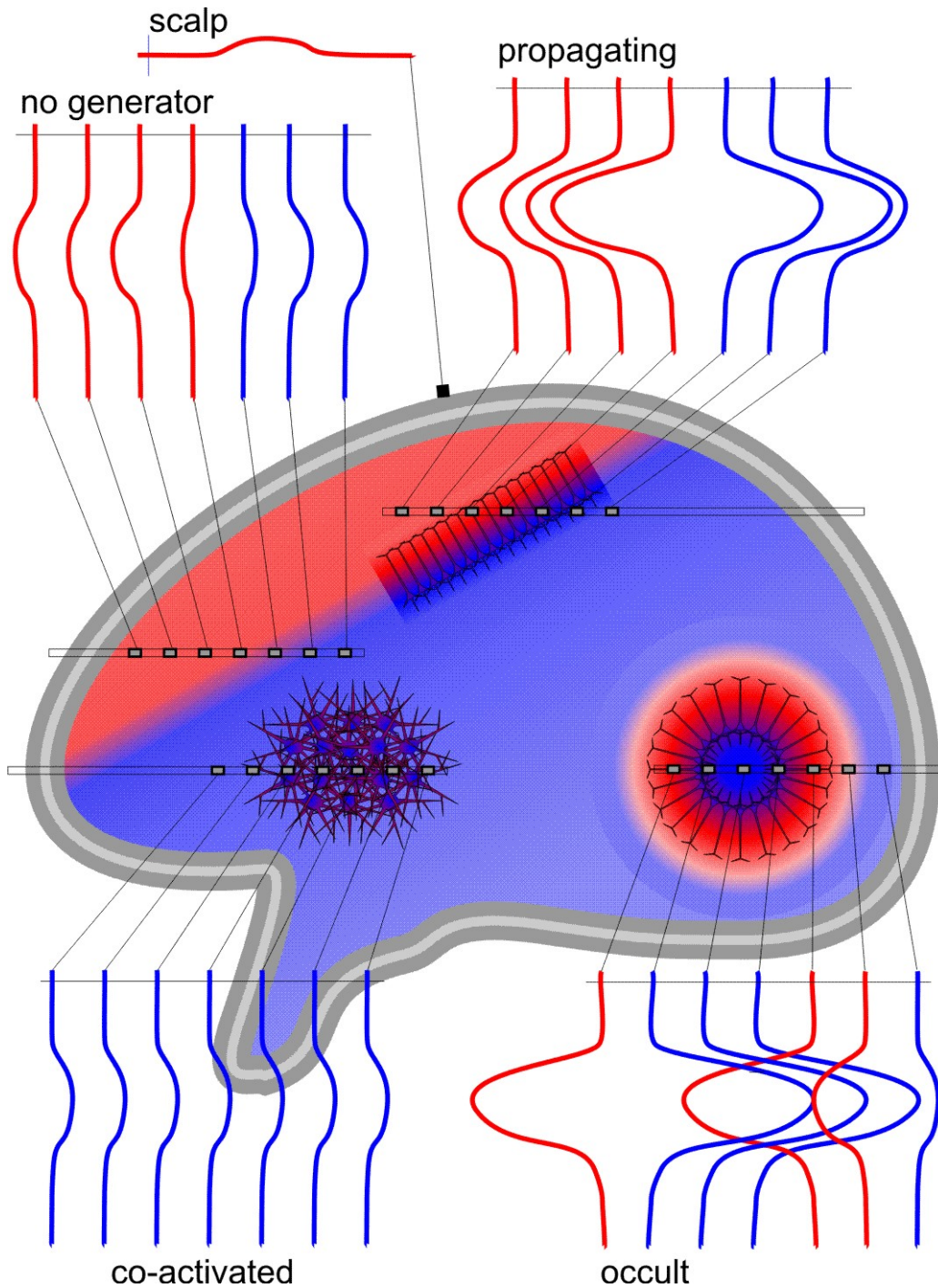


**Figure 2. Complex Relationships between Brain Activity and Scalp Recordings.** The *propagating* generator is composed of cells like that illustrated in fig. 1, aligned in an open field. Their net activity is recorded at the scalp, but many inverse methods would mis-estimate the location and extent of the source. A depth electrode penetrating the generator would record large inverting potentials, as it would within the *occult* generator. However, the different parts of the occult generator cancel one another, and no field escapes to the scalp. An electrode passing where there is *no generator* may also record inverting potentials, but they will be smaller and with more gradual gradients. Because actual P3 generators are likely to be extended, and cortex is highly convoluted, recordings within actual generators are likely to show multiple inversions and/or reversing gradients. The *co-activated* neurons receive the same synaptic input as the propagating and occult cells, but they lack the morphological and spatial organization necessary to generate even a local P3, although increased synaptic activity may be reflected in high gamma power. Note that even a perfect inverse solution would not localize the co-activated or occult generators.

### **Validation of non-invasive source localization with iEEG**

Like MEG and scalp-EEG, iEEG has a very high temporal resolution (<1ms) and a direct relation to synaptic communication. Unlike MEG or scalp-EEG, iEEG also has very high spatial resolution (effectively limited only by electrode size and spacing), and is the only method that can unambiguously identify ERP generators. However, iEEG has four serious limitations: pathological contamination, limited sampling, unclear contribution to extracerebral M/EEG, and susceptibility to volume conduction.

Depth electrodes are only implanted for strictly clinical purposes in epileptic subjects for the purpose of localizing their epileptic focus prior to its surgical removal [69]. During the time that the patients are waiting for the arrival of a spontaneous seizure, they may consent to perform cognitive tasks while their relatively normal brain regions are recorded. In most cases, epileptogenic pathology attenuates the local cognitive potentials [70-75]. However, occasionally, epileptiform hyper-responsiveness can also be observed [76,77]. Nonetheless, it is possible to select for study patients who perform cognitive tasks in the normal range, and who produce normal scalp cognitive EPs. Furthermore, epileptiform activity is localized in time and space, and so it is possible to select patients, sites and epochs for analyses that appear electrographically normal.

A second limitation of depth recordings is that they provide unambiguous localizing information only in a small region surrounding the electrode contact, and in a given patient, electrodes are only implanted into a limited region. The great advantage of intracranial electrodes is their high spatial resolution, but this necessarily also implies that they will usually miss activity if they do not directly sample the active area. One can estimate that the ~100 recording sites in any given patient would sample high amplitude cognitive activity from ~10% of the brain. Thus, the choice of recording sites has a profound effect on what can be observed. In particular, due to their common involvement in epileptogenesis and the existence of a safe surgical approach, the hippocampus and amygdala have been recorded from more than any other brain area. Conversely, certain brain regions remain undersampled, because they are seldom involved in epileptogenesis and/or they are difficult to approach surgically. Poorly sampled regions include the insular/opercular cortices, and the most dorsal parietal, posterior occipital, and anterior frontal cortices. However, this limitation has largely been overcome for the P3 due to the large number of electrode contacts sampled in different regions, across surgical programs with different clinical strategies.

A third limitation of iEEG is that evaluating the possible contribution of a demonstrated local EP generator to the extracerebral M/EEG field is complicated, requiring an accurate computational forward model that incorporates knowledge of: (1) the detailed spatial configuration of all dipoles within the generating cortex; (2) the strength and timing of each dipole; and (3) the 3D distribution of tissues with different impedances in the head. Due to the limited sampling of iEEG, this ideal has never been realized, the exact relation between the generators of cognitive EPs, and those recorded at the scalp, remains unclear.

A critical test for whether a particular depth-P3 generator contributes to the scalp-P3 is provided by scalp recordings after a lesion in that generator [78]. However, interpretation of such studies is not necessarily straightforward (fig. 2) [79]. Clearly, destruction of a propagating generator would usually be expected to diminish the corresponding scalp-P3 component. However, it is difficult to evaluate the possible influences of the removal of 'cancelling' generators (which could even result in a post-lesional increase in amplitude). For example, if the local depth-P3 is positive at the local cortical surface, then lesions of the orbital surface would mainly remove dipoles pointing in the 'wrong way,' and thus result in an increased scalp-P3. Conversely, lesions of locations that do not generate depth-P3s may still decrease the scalp-P3 if they disrupt antecedent processes that must occur prior to activation of the actual generating structures. For example, frontal areas may perform executive processes that are essential before working memory is updated, but the actual updating may occur elsewhere and give rise directly to the P3. While the most likely interpretation of a lesion-induced decreased scalp-P3 as indicating that the lesioned structure contains P3 generators may usually be correct, other possibilities should be borne in mind.

Passive propagation of EEG and thus far-field recordings also occur intracranially (fig. 2). Consequently, simply recording a potential intracranially does not establish its local generation. Even inversions can be recorded at a distance, for example as one passes through the iso-electric plane of a simple dipolar source. Conversely, one may be in an active generator, but because of superimposed potentials from distant sources, not observe an inversion in polarity locally. Working from basic principles, Nicholson and Freeman [2] demonstrated how transmembrane currents can be localized in three dimensions using the second spatial derivative of the potential, taking into account the local conductivities. Although this method is usually applied to microelectrode array recordings, the same principles apply to depth macroelectrode recordings, with steep and changing voltage gradients indicating local generation. Again, these signs must be interpreted with reference to the local conductivity profile as this can greatly influence current flows and thus voltage gradients. Local generation is also indicated if the local potentials are larger than in all surrounding structures. An indirect but strong indicator of local generation is changes in cell-firing that are correlated in time and cognitive correlates with local field potentials, since action potentials do not propagate significantly for reasons discussed above [80]. Application of these multiple criteria to demonstrate local generation is rare, but has occurred for the P3b in the hippocampal formation, where



steep voltage gradients, changes in cell-firing, and larger amplitude than surrounding structures in all directions have all been demonstrated (see companion chapter by Halgren). None of these criteria can be completely satisfied using subdural strips or grids. In such cases, local generation is inferred from relatively large local amplitude in two dimensions. This limitation of iEEG strikes to the heart of its utility, and emphasizes the need to develop quantitative methods to infer generator localization from the sampled electrical field using conductivities inferred from cerebral segmentation [81] and diffusion tensor imaging [82].

Despite these limitations, intracranial recording is the only method that is capable of demonstrating local generation unambiguously. It is thus of interest to compare the localization of intracranial P3 generators as inferred from BOLD with the results of iEEG (for review see [83]). Although there is a general correspondence when comparing across studies [84,85], there is only partial correspondence of P3 source localization from simultaneous BOLD and scalp EEG recordings compared to the intracranial results described in the companion chapter by Halgren [86,87]. Significantly, the only direct within-subject comparison of iEEG and BOLD localization of the P3 found clear dissociations [88]. However, rapid progress in simultaneous scalp-EEG/BOLD recording, and signal-separation/source-estimation is yielding increasing convergence with iEEG-derived generator structures.

## Conclusions

In this review, we have seen that by itself, each measure can provide only limited knowledge of the underlying P3 process. Before neuronal currents can be recorded extracranially as EEG and MEG, they must spatiotemporally summate. Most do not and so remain invisible. Localizing those currents that do propagate requires prior assumptions that are problematic for the P3. Unlike EEG and MEG, intracranial EEG is not inherently ambiguous, but is limited by possible influences of pathology and incomplete sampling. BOLD is limited in its temporal resolution and has poor signal to noise in important P3b generators. Combining across techniques can help overcome these limitations, but even accurate identification of the neural structures generating the P3s has limited implications for the mechanisms whereby they modulate cerebral information processing. Bringing the P3s and the cognitive states that they embody into mechanistic neuroscience requires understanding at the synaptic, cellular and circuit level, rather than the structure level of BOLD and macro-iEEG.

## Acknowledgements

Supported by USPHS NS18741 and NS44623. Thanks to A. Dale and M. Huang for collaboration in the studies reported here. Correspondence to: Eric Halgren, Multimodal Imaging Laboratory, 9500 Gilman Drive, La Jolla, CA 92093-0841, email: ehalgren@ucsd.edu

## References

1. Hamalainen M, Hari R, Ilmoniemi RJ, Knuutila J, Lounasmaa OV. Magnetoencephalography - theory, instrumentation, and application to noninvasive studies of the working human brain. *Reviews of Modern Physics* 1993; 65:413-97.
2. Nicholson C, Freeman JA. Theory of current source density analysis and determination of the conductivity tensor for anuran cerebellum. *Journal of Neurophysiology* 1975; 38:356-68.
3. Liu AK, Belliveau JW, Dale AM. Spatiotemporal imaging of human brain activity using fMRI constrained MEG data: Monte Carlo simulations. *Proceedings of the National Academy of Sciences of the United States of America* 1998; 95:8945-50.
4. Sharon D, Hamalainen MS, Tootell RB, Halgren E, Belliveau JW. The advantage of combining MEG and EEG: comparison to fMRI in focally stimulated visual cortex. *Neuroimage* 2007; 36:1225-35.
5. Attwell D, Laughlin SB. An energy budget for signaling in the grey matter of the brain. *J Cereb Blood Flow Metab* 2001; 21:1133-45.
6. Hille B. *Ion Channels of Excitable Membranes*. Sunderland, MA: Sinauer, 2001.
7. Humphrey DR. Re-analysis of the antidromic cortical response. II. On the contribution of cell discharge and PSPs to the evoked potentials. *Electroencephalogr Clin Neurophysiol* 1968; 25:421-42.
8. Okada Y, Ikeda I, Zhang T, Wang Y. High-frequency signals (> 400 Hz): a new window in electrophysiological analysis of the somatosensory system. *Clin EEG Neurosci* 2005; 36:285-92.
9. Mitzdorf U. Current source-density method and application in cat cerebral cortex: investigation of evoked potentials and EEG phenomena. *Physiol Rev* 1985; 65:37-100.
10. Destexhe A, Rudolph M, Pare D. The high-conductance state of neocortical neurons in vivo. *Nat Rev Neurosci* 2003; 4:739-51.
11. Shao Z, Burkhalter A. Different balance of excitation and inhibition in forward and feedback circuits of rat visual cortex. *J Neurosci* 1996; 16:7353-65.
12. Cunningham MO, Pervouchine DD, Racca C, et al. Neuronal metabolism governs cortical network response state. *Proc Natl Acad Sci U S A* 2006; 103:5597-601.
13. Kandel ER, Spencer WA, Brinley FJ, Jr. Transient and long-lasting electrical responses to direct hippocampal stimulation. *Am J Physiol* 1960; 198:687-92.
14. Gonchar Y, Burkhalter A. Distinct GABAergic targets of feedforward and feedback connections between lower and higher areas of rat visual cortex. *J Neurosci* 2003; 23:10904-12.
15. Lai HC, Jan LY. The distribution and targeting of neuronal voltage-gated ion channels. *Nat Rev Neurosci* 2006; 7:548-62.
16. Murakami S, Zhang T, Hirose A, Okada YC. Physiological origins of evoked magnetic fields and extracellular field potentials produced by guinea-pig CA3 hippocampal slices. *J Physiol* 2002; 544:237-51.

17. Murakami S, Hirose A, Okada YC. Contribution of ionic currents to magnetoencephalography (MEG) and electroencephalography (EEG) signals generated by guinea-pig CA3 slices. *J Physiol* 2003; 553:975-85.
18. Traub R, Miles R. *Neuronal Networks of the Hippocampus*. Cambridge: University Press, 1991.
19. Einevoll GT, Pettersen KH, Devor A, Ulbert I, Halgren E, Dale AM. Laminar Population Analysis: Estimating firing rates and evoked synaptic activity from multielectrode recordings in rat barrel cortex. *J Neurophysiol* 2006.
20. Felleman DJ, VanEssen DC. Distributed hierarchical processing in the primate cerebral cortex. *Cereb Cortex* 1991; 1:1-47.
21. Barbas H, Rempel-Clover N. Cortical structure predicts the pattern of corticocortical connections. *Cereb Cortex* 1997; 7:635-46.
22. Thomson AM, Bannister AP. Interlaminar connections in the neocortex. *Cereb Cortex* 2003; 13:5-14.
23. Jones EG. Thalamic circuitry and thalamocortical synchrony. *Philos Trans R Soc Lond B Biol Sci* 2002; 357:1659-73.
24. Casanova MF, Trippe J, 2nd. Regulatory mechanisms of cortical laminar development. *Brain Res Rev* 2006; 51:72-84.
25. Stapleton JM, Halgren E, Moreno KA. Endogenous potentials after anterior temporal lobectomy. *Neuropsychol* 1987; 25:549-57.
26. Rugg MD, Pickles CD, Potter DD, Roberts RC. Normal P300 following extensive damage to the left medial temporal lobe. *Journal of Neurology, Neurosurgery and Psychiatry* 1991; 54:217-22.
27. Onofrij M, Fulgente T, Nobilio D, et al. P3 recordings in patients with bilateral temporal lobe lesions. *Neurology* 1992; 42:1762-7.
28. Polich J, Squire LR. P300 from amnesic patients with bilateral hippocampal lesions. *Electroencephalography and Clinical Neurophysiology* 1993; 86:408-17.
29. Nunez PL. The brain's magnetic field: some effects of multiple sources on localization methods. *Electroencephalography and Clinical Neurophysiology* 1986; 63:75-82.
30. Ary JP, Darcey TM, Fender DH. Locating electrical sources in the human brain. *IEEE Transactions on Biomedical Engineering* 1981; 28:1-5.
31. Pelizzone M, Hari R. Interpretation of neuromagnetic responses: two simple models for extended current sources in the human auditory cortex. *Acta Otolaryngologica (Stockholm)* 1986; Suppl. 432:15-20.
32. Lutkenhoner B. Magnetoencephalography and its Achilles' heel. *J Physiol Paris* 2003; 97:641-58.
33. Cohen D, Cuffin BN. Demonstration of useful differences between magnetoencephalogram and electroencephalogram. *Electroencephalography and Clinical Neurophysiology* 1983; 56:38-51.
34. Hillebrand A, Barnes GR. A quantitative assessment of the sensitivity of whole-head MEG to activity in the adult human cortex. *Neuroimage* 2002; 16:638-50.
35. Nunez PL, Silberstein RB. On the relationship of synaptic activity to macroscopic measurements: does co-registration of EEG with fMRI make sense? *Brain Topogr* 2000; 13:79-96.
36. Helmholtz H. Ueber einige Gesetze der Vertheilung elektrischer Strome in körperlichen Leitern, mit Anwendung auf die thierisch-elektrischen Versuche [Some laws concerning the distribution of electric currents in volume conductors with applications to experiments on animal electricity]. *Ann Phys Chem* 1853; 89:211-33, 353-77.
37. Devor A, Tian P, Nishimura N, et al. Suppressed neuronal activity and concurrent arteriolar vasoconstriction may explain negative blood oxygenation level-dependent signal. *J Neurosci* 2007; 27:4452-9.
38. Shmuel A, Augath M, Oeltermann A, Logothetis NK. Negative functional MRI response correlates with decreases in neuronal activity in monkey visual area V1. *Nat Neurosci* 2006; 9:569-77.
39. Lauritzen M. Reading vascular changes in brain imaging: is dendritic calcium the key? *Nat Rev Neurosci* 2005; 6:77-85.
40. Attwell D, Iadecola C. The neural basis of functional brain imaging signals. *Trends Neurosci* 2002; 25:621-5.
41. Mintun MA, Lundstrom BN, Snyder AZ, Vlassenko AG, Shulman GL, Raichle ME. Blood flow and oxygen delivery to human brain during functional activity: theoretical modeling and experimental data. *Proc Natl Acad Sci U S A* 2001; 98:6859-64.
42. Hamel E. Perivascular nerves and the regulation of cerebrovascular tone. *J Appl Physiol* 2006; 100:1059-64.
43. Cauli B, Tong XK, Rancillac A, et al. Cortical GABA interneurons in neurovascular coupling: relays for subcortical vasoactive pathways. *J Neurosci* 2004; 24:8940-9.
44. Woolsey TA, Rovainen CM, Cox SB, et al. Neuronal units linked to microvascular modules in cerebral cortex: Response elements for imaging the brain. *Cereb Cortex* 1996; 6:647-60.
45. Raichle ME. Circulatory and metabolic correlates of brain function in normal humans. In: Plum F, (editor). *Handbook of Physiology. The Nervous System V, Higher Functions of the Brain* Bethesda, MD: Amer Physiol Soc; 1987: pp. 643-74.
46. Nunez PL. *Electric Fields of the Brain*. New York: Oxford University 1981.
47. Steriade M, Amzica F. Slow sleep oscillation, rhythmic K-complexes, and their paroxysmal developments. *Journal of Sleep Research* 1998; 7:30-5.
48. Maquet P, Phillips C. Functional brain imaging of human sleep. *Journal of Sleep Research* 1998; 7:42-7.
49. Fernandez-Seara MA, Wang J, Wang Z, et al. Imaging mesial temporal lobe activation during scene encoding: Comparison of fMRI using BOLD and arterial spin labeling. *Hum Brain Mapp* 2007; 28:1391-400.
50. Bellgowan PS, Bandettini PA, van Gelderen P, Martin A, Bodurka J. Improved BOLD detection in the medial temporal region using parallel imaging and voxel volume reduction. *Neuroimage* 2006; 29:1244-51.
51. Sherg M, VonCramon D. Two bilateral sources of the late AEP as identified by a spatio-temporal dipole model. *Electroencephalography and Clinical Neurophysiology* 1985; 62:32-44.
52. Halgren E, Marinkovic K, Chauvel P. Generators of the late cognitive potentials in auditory and visual oddball tasks. *Electroencephalogr Clin Neurophysiol* 1998; 106:156-64.
53. Halgren E, Baudena P, Heit G, Clarke JM, Marinkovic K, Chauvel P. Spatio-temporal stages in face and word processing. 2. Depth-recorded potentials in the human frontal and Rolandic cortices. *Journal of Physiology (Paris)* 1994; 88:51-80.
54. Halgren E, Baudena P, Heit G, Clarke JM, Marinkovic K. Spatio-temporal stages in face and word processing. 1. Depth-recorded potentials in the human occipital, temporal and parietal lobes. *Journal of Physiology (Paris)* 1994; 88:1-50.
55. Clarke JM, Halgren E, Chauvel P. Intracranial ERP recordings in humans during a lateralized visual oddball task: 1. Occipital and perirolandic recordings. *Clinical Neurophysiology* 1999; 110:1210-25.
56. Clarke JM, Halgren E, Chauvel P. Intracranial ERP recordings during a lateralized visual oddball task: 2. temporal, parietal and

- frontal recordings. *Electroencephalography and Clinical Neurophysiology* 1999; 110:1226-44.
57. Kiehl KA, Stevens MC, Laurens KR, Pearlson G, Calhoun VD, Liddle PF. An adaptive reflexive processing model of neurocognitive function: Supporting evidence from a large scale (n=100) fMRI study of an auditory oddball task. *NeuroImage* 2005; 25:899-915.
  58. Dale AM, Halgren E. Spatiotemporal mapping of brain activity by integration of multiple imaging modalities. *Current Opinion in Neurobiology* 2001; 11:202-8.
  59. Uutela K, Hamalainen M, Somersalo E. Visualization of magnetoencephalographic data using minimum current estimates. *Neuroimage* 1999; 10:173-80.
  60. Huang MX, Dale AM, Song T, et al. Vector-based spatial-temporal minimum L1-norm solution for MEG. *Neuroimage* 2006; 31:1025-37.
  61. Dale AM, Liu AK, Fischl BR, et al. Dynamic statistical parametric mapping: combining fMRI and MEG for high-resolution imaging of cortical activity. *Neuron* 2000; 26:55-67.
  62. Wagner M, Fuchs M, Kastner J. Evaluation of sLORETA in the presence of noise and multiple sources. *Brain Topography* 2004; 16:277-80.
  63. Hillebrand A, Singh KD, Holliday IE, Furlong PL, Barnes GR. A new approach to neuroimaging with magnetoencephalography. *Hum Brain Mapp* 2005; 25:199-211.
  64. Makeig S, Bell AJ, Jung TP, Sejnowski TJ. Independent component analysis of electroencephalographic data. In: Touretzky D, Mozer M, Hasselmo M, (editors). *Advances in Neural Information Processing Systems 8* Cambridge, MA: MIT Press; 1996: pp. 145-51.
  65. Mosher JC, Baillet S, Leahy RM. EEG source localization and imaging using multiple signal classification approaches. *J Clin Neurophysiol* 1999; 16:225-38.
  66. Kayser J, Tenke CE. Trusting in or breaking with convention: towards a renaissance of principal components analysis in electrophysiology. *Clin Neurophysiol* 2005; 116:1747-53.
  67. Bullock T, McClune M, Achimowicz J, Iragui-Madoz V, Duckrow R, Spencer S. EEG coherence has structure in the millimeter domain: subdural and hippocampal recordings from epileptic patients. *Electroencephalography and Clinical Neurophysiology* 1995; 95:161-77.
  68. Klopp JC, Halgren E, Marinkovic K, Nenov VI. Face specific wide-spread wide-band intracranial EEG coherence in humans. In Society for Neuroscience Abstracts. 1998. p. 1762.
  69. Chauvel P, Vignal JP, Biraben A, Badier JM, Scarabin JM. Stereo-electroencephalography. In: Pawlik G, Stefan H, (editors). *Multimethodological assessment of the localization-related epilepsy*: Springer Verlag; 1996: pp. 135-63.
  70. Squires NK, Halgren E, Wilson CL, Crandall PH. Human endogenous limbic potentials: Cross-modality and depth/surface comparisons in epileptic subjects. In: Gaillard AWK, Ritter W, (editors). *Tutorials in ERP Research: Endogenous Components* Amsterdam: North Holland; 1983: pp. 217-32.
  71. McCarthy G, Darcey TM, Wood CC, Williamson PD, Spencer DD. Asymmetries in scalp and intracranial endogenous ERPs in patients with complex partial epilepsy. In: Engel J, Ojemann G, Luders H, Williamson PD, (editors). *Fundamental Mechanisms of Human Brain Function* New York: Raven; 1987: pp. 51-59.
  72. Wood CC, McCarthy G, Kim JH, Spencer DD, Williamson PD. Abnormalities in temporal lobe event-related potentials predict hippocampal cell loss in temporal lobe epilepsy. *Society for Neuroscience Abstracts* 1988; 14:5.
  73. Meador KJ, Loring DW, King DW, et al. Limbic evoked potentials predict site of epileptic focus. *Neurology* 1989; 37:494-97.
  74. Puce A, Kalnins RM, Berkovic SF, Donnan GA, Bladin PF. Limbic P3 potentials, seizure localization, and surgical pathology in temporal lobe epilepsy. *Annals of Neurology* 1989; 26:377-85.
  75. Halgren E, Stapleton J, Domalski P, et al. Memory dysfunction in epileptics as a derangement of normal physiology. *Advances in Neurology* 1991; 55:385-410.
  76. Altafullah I, Halgren E. Focal medial temporal lobe spike-wave complexes evoked by a memory task. *Epilepsia* 1988; 29:8-13.
  77. Clarke JM, Halgren E, Scarabin JM, Chauvel P. Auditory and visual sensory representations in human prefrontal cortex as revealed by stimulus-evoked spike-wave complexes. *Brain* 1995; 118:473-84.
  78. Soltani M, Knight RT. Neural origins of the P300. *Crit Rev Neurobiol* 2000; 14:199-224.
  79. Halgren E, Stapleton JM, Smith ME, Altafullah I. Generators of the human scalp P3s. In: Cracco RQ, Bodis-Wollner I, (editors). *Evoked Potentials* New York: Liss; 1986: pp. 269-89.
  80. Grover FS, Buchwald JS. Correlation of cell size with amplitude of background fast activity in specific brain nuclei. *J Neurophysiol* 1970; 33:160-71.
  81. Fischl B, Salat DH, Busa E, et al. Whole brain segmentation. Automated labeling of neuroanatomical structures in the human brain. *Neuron* 2002; 33:341-55.
  82. Tuch DS, Wedeen, V.J., Dale, A.M., George, J.S., and Belliveau, J.W. Conductivity tensor mapping of the human brain using diffusion tensor MRI. *Proc Natl Acad Sci U S A* 2001; in press.
  83. Linden DEJ. The P300: Where in the brain is it produced and what does it tell us? *The Neuroscientist* 2005; 11:563-76.
  84. McCarthy G, Luby M, Gore J, Goldman-Rakic P. Infrequent events transiently activate human prefrontal and parietal cortex as measured by functional MRI. *J Neurophysiol* 1997; 77:1630-4.
  85. Bledowski C, Prvulovic D, Hoehstetter K, et al. Localizing P300 generators in visual target and distractor processing: a combined event-related potential and functional magnetic resonance imaging study. *J Neurosci* 2004; 24:9353-60.
  86. Benar CG, Schon D, Grimault S, et al. Single-trial analysis of oddball event-related potentials in simultaneous EEG-fMRI. *Hum Brain Mapp* 2007; 28:602-13.
  87. Eichele T, Specht K, Moosmann M, et al. Assessing the spatiotemporal evolution of neuronal activation with single-trial event-related potentials and functional MRI. *Proc Natl Acad Sci U S A* 2005; 102:17798-803.
  88. Brazdil M, Dobsik M, Mikl M, et al. Combined event-related fMRI and intracerebral ERP study of an auditory oddball task. *Neuroimage* 2005; 26:285-93.